α decay of excited states in ^{14}C

D. L. Price,[1] M. Freer,[1] N. I. Ashwood,[1] N. M. Clarke,[1] N. Curtis,[1] L. Giot,[2] V. Lima,[3] P. Mc Ewan,[1] B. Novatski,[4] N. A. Orr,[2] S. Sakuta,[4] J. A. Scarpaci,[3] D. Stepanov,[4] and V. Ziman[1]

[1]*School of Physics and Astronomy, University of Birmingham, Edgbaston, Birmingham B15 2TT, United Kingdom*

[2]*LPC-ENSICAEN, IN2P3-CNRS et Université de Caen, F-14050 Caen Cedex, France*

[3]*Institut de Physique Nucléaire d'Orsay, rue Georges Clemenceau, F-91406 Orsay Cedex, France*

[4]*RRC "Kurchatov Institute," Kurchatov sq.1, RU-123182 Moscow, Russia*

(Received 24 October 2006; published 4 January 2007)

Measurements of the ^{14}C(^{14}C,^{14}C[^{10}Be + α]) breakup reaction have been made at a beam energy of 98.2 MeV. The studies were performed with two charged-particle telescopes that permitted the energy, mass, charge, and emission angle of each detected particle to be determined. A series of ^{14}C excited states at energies of 14.3, 14.8 15.6, 16.4, 17.3, 18.6, 19.8, 20.6, and 21.6 MeV was observed to decay to either the ^{10}Be ground state or the first excited states. Angular correlation measurements suggest an assignment of $J^{\pi} = 3^{-}$ for the 15.6 MeV state.

DOI: 10.1103/PhysRevC.75.014305 PACS number(s): 21.60.Gx, 23.20.En, 25.70.Ef, 27.20.+n

I. INTRODUCTION

It is a long-standing belief that the α particle strongly influences the structure of light nuclei. In certain instances it has been suggested that the nucleus can condense into an ensemble of α clusters. The influence of valence neutrons on the stability of these cluster structures is intriguing. For instance it has been proposed that neutrons occupy covalent orbits stabilizing the cluster structures against bending modes [1].

The carbon isotopes are an interesting case. The ^{12}C nucleus may be described in terms of a geometric arrangements of three α particles. The 7.65 MeV 0^{+} state has been identified as a low density α-cluster state, possibly with properties that are analogous to a Bose gas, or even condensate [2]. The location of the linear cluster configuration remains a question of some debate, but it may be associated with the 10.3 MeV 0^{+} state that has been the subject of recent investigation [3]. Alternatively, this state may be a monopole excitation of the gas state.

The fact that no clear experimental signature has emerged for such a linear-chain state may be related to the intrinsic instability of such an arrangement against the collapse into more stable structures. Calculations by Itagaki *et al.* [4] do in fact demonstrate this instability and, moreover, demonstrate that the linear chains may be stabilized in the neutron-rich carbon isotopes by the presence of the valence neutrons. These ideas have been explored extensively by Milin, von Oertzen, and collaborators, in two papers on ^{13}C [5] and ^{14}C [6], by attempting to eliminate states in these nuclei associated with shell-model-like single-particle states and then assigning the remaining states to rotational bands they proposed for prolate (linear chain) and oblate (triangular) cluster structures in ^{13,14}C.

However, many of the states involved in this analysis are not well understood. In particular the spin and parity assignments are uncertain, and further measurements are required to confirm their character. The proposed cluster bands should exhibit a strong α decay, and recent measurements of the α decay of ^{13}C and ^{14}C have produced results that are not entirely consistent with the earlier interpretation [7]. Thus, it is clear that more experimental information is required to fix the properties of these states.

Here we present measurements of the α decay of ^{14}C observed in the ^{14}C(^{14}C,^{14}C[^{10}Be + α]) reaction in which we measure the spin of one of the α-decaying excited states in ^{14}C in this region of great interest.

II. EXPERIMENTAL DETAILS

The measurements were performed using the Tandem accelerator facility at IPN-Orsay, France. An 80% enriched ^{14}C (280 μg/cm^2) target was bombarded with a ^{14}C beam at an energy of 98.2 MeV. The beam exposure was 1.09 mC, with typical beam intensities of 7 to 10 enA.

The charged breakup fragments produced in the reactions were detected by two forward-mounted telescopes (at $\pm 17.0^{\circ}$ with the beam axis) each consisting of three elements. The position-sensitive elements of both telescopes were located at a distance of 149 mm from the target. The first element of each telescope was a silicon detector with an area of 50×50 mm^2 and a thickness of 70 μm. These were subdivided into quadrants each 25×25 mm^2 to reduce the detector capacitance and thus improve the energy resolution. The second element was position-sensitive silicon strip detectors with an area of 50×50 mm^2 and a thickness of 500 μm. These possessed 16 strips, each 3 mm wide, separated by 0.13 mm and covering the entire width of the active area. The strips were aligned in the horizontal plane, i.e., with the position-sensitive axis directed toward the beam axis (the z axis). The final elements of the telescopes were 50×50 mm^2, 1-cm-thick CsI scintillation detectors.

Calibration of the telescopes was performed using a combination of direct exposure to a three-line α source (^{239}Pu, 5.155 MeV; ^{241}Am, 5.488 MeV; and ^{244}Cm, 5.805 MeV) and by elastically scattering a ^{14}C beam at 43.7 MeV from a ^{208}Pb target. Measurements were made without the first silicon detectors *in situ* to provide an accurate, and independent, calibration of the silicon strip detectors. The energy resolution of the telescopes was dominated by the silicon strip detectors

with a resolution of 300 keV. The position resolution along the strip (x direction) was <1 mm, and 1.5 mm in the y direction, as defined by the strip width. These telescopes provided information on the mass, charge, energy, and emission angle of each detected particle.

III. ANALYSIS AND RESULTS

The detection system permitted the determination of the direction and energy (and hence momentum) of the ^{14}C breakup products. As the recoil particle was not detected, momentum conservation was used to provide a complete reconstruction of the reaction kinematics. To obtain a clean separation of reaction channels, particle identification was of prime importance. A plot of the energy detected in the strip detectors (E) against the energy detected in the quadrant detectors ($\triangle E$) provided particle identification (Fig. 1).

Analysis was performed of the breakup of the excited ^{14}C nuclei into $^{10}\mathrm{Be}+\alpha$ at forward angles in the projectile-target center-of-mass frame. Here the dominant excitation mechanism was expected to be inelastic scattering. The momentum of the recoil particle was deduced from the difference in momentum of the beam and the two detected fragments. Thus, the kinetic energy of the unobserved recoil could be determined. This allowed a calculation of the total final state kinetic energy (E_{tot}), which is related to the reaction Q value via

$$Q = E_{\mathrm{tot}} - E_{\mathrm{beam}}. \tag{1}$$

A total energy spectrum therefore reveals the states of the three final state particles.

Figure 2 shows the total energy spectrum obtained after coincident detection of ^{10}Be and α particles (the ^{10}Be and α particles being detected on opposite sides of the beam axis), assuming a ^{14}C recoil. The strong peak at 86.2 MeV corresponds to events in which all of the particles are emitted in their ground states and is consistent with the reaction Q value

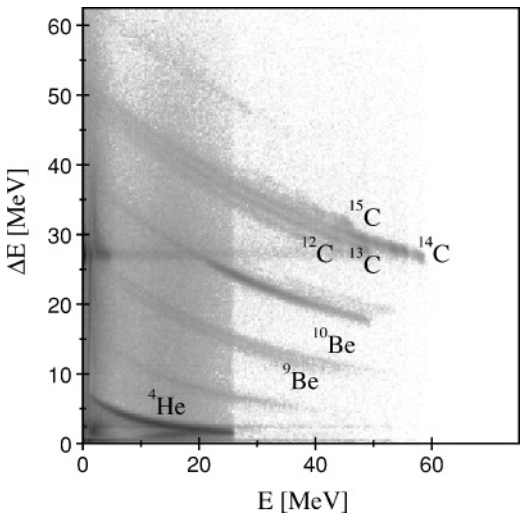

FIG. 1. Particle identification plot. The vertical stripe at $E \leqslant 25$ MeV corresponds to the coincident detection of uncorrelated α particles.

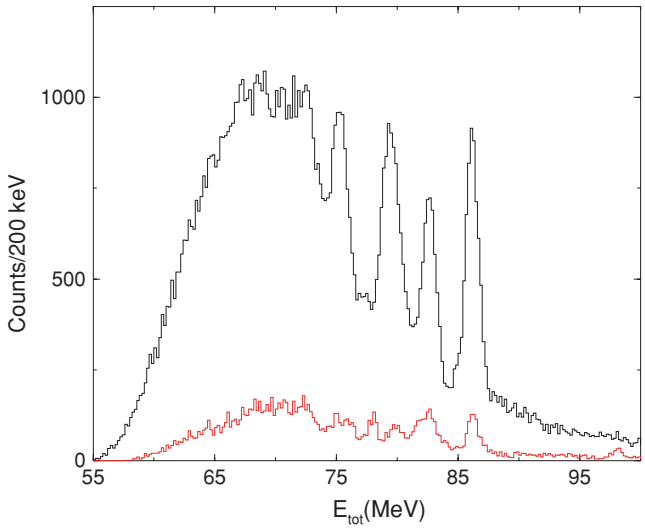

FIG. 2. (Color online) Total final state kinetic energy (E_{tot}) for the $^{14}\mathrm{C}(^{14}\mathrm{C},^{10}\mathrm{Be}+\alpha)^{14}\mathrm{C}$ reaction at a beam energy of 98.2 MeV. The spectrum indicated by the red histogram corresponds to the $^{12}\mathrm{C}(^{14}\mathrm{C},^{10}\mathrm{Be}+\alpha)^{12}\mathrm{C}$ reaction measured with the natural carbon target. This latter spectrum has been scaled such that it corresponds to the expected ^{12}C component in the ^{14}C target.

of -12.011 MeV. The resolution with which the total energy is reconstructed was 1.4 MeV (FWHM), which is typical for such measurements [8]. The peak observed at a total energy of 82.8 MeV corresponds to events where the ^{10}Be is emitted in the 3.36 (2^+) MeV first excited state. Owing to the much higher energy of the first excited states in ^{4}He (20.21 MeV) and ^{14}C (6.09 MeV) this peak cannot correspond to events in which either of these particles are in an excited state. The peak observed at the total energy of 79.4 MeV (i.e., 6.8 MeV less than the highest energy peak) is most probably a combination of excitations of several states, when either the ^{10}Be or the recoiling ^{14}C nucleus is excited (we return to this point later). It is also observed that the width of this peak is larger than the two higher energy peaks, which is consistent with this interpretation. In particular, the ^{14}C states at 6.09 (1^-), 6.59 (0^+), 6.73 (3^-), 6.90 (0^-), and 7.01 MeV (2^+) and the four ^{10}Be states at $\sim$6 MeV are expected to contribute. There is one further peak in the total energy spectrum, which appears at an energy of 10.8 MeV below the peak corresponding to production of all the nuclei in their ground states. It is proposed that this peak coincides with excitation of the ^{14}C recoil to the states listed above, together with the ^{10}Be being emitted in the first excited state. Separate measurements were performed with a natural carbon target. These measurements confirmed that the contaminant ^{12}C contributions to the total energy spectrum in Fig. 2 are small. The spectrum from the measurements with the natural carbon target is shown. There is a spectrum of peaks in this spectrum, but it is observed that these are different from those arising from the ^{14}C target. Particularly, the peak close to 82 MeV is broader than that for the ^{14}C target because of the presence of the 4.4 MeV ^{12}C recoil excitation. Moreover, the lower total energy peaks at 77–80 MeV are found not to coincide with the strong peak in the ^{14}C target data. This would

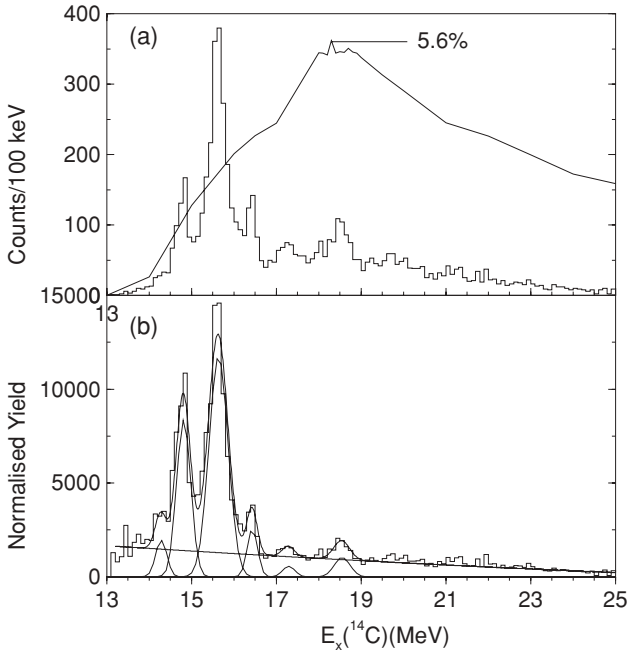

FIG. 3. (a) ^{14}C excitation energy spectrum for the decay to ^{10}Be + α, measured at a beam energy of 98.2 MeV. The solid line corresponds to the variation in detection efficiency with excitation energy, as calculated using Monte Carlo simulations. The maximum detection efficiency is indicated. (b) The excitation energy spectrum corrected for the variation in detection efficiency to give normalized yield. Fits to the peaks are also shown, together with an indication of the background.

also imply that the high energy side of the peak at 79.4 MeV corresponds to excited states in ^{10}Be, whereas the lower energy side is dominated by contributions from the ^{14}C recoil.

By gating on the peak corresponding to the three final state particles being produced in their ground states the excitation energy of the breakup particle can be determined from the relative velocity of the two decay products. The corresponding ^{14}C excitation energy spectrum is displayed in Fig. 3 and shows evidence for peaks ranging in excitation energy from 14.3 to 18.6 MeV. The decay to the ^{10}Be ground state shows evidence for states at E_x=14.3, 14.8, 15.6, 16.4, 17.3, and 18.6 MeV, with possibly a further state at 18.1 MeV.

To compensate for the fact that the experimental detection efficiency varies strongly with excitation energy, Monte Carlo simulations were performed. These simulations include the details of the detector geometry and energy thresholds, together with those of the reaction kinematics. The angular distribution of the inelastically scattered ^{14}C was assumed to have an exponential form, whilst the emission of the breakup products was assumed to be isotropic. The resulting efficiency profile is shown in Fig. 3(a). The experimental excitation energy spectrum is shown normalized for the variation in detection efficiency in Fig. 3(b). It is the latter spectrum from which the energy centroids have been extracted, as listed in Table I. It is possible to determine the excitation energy resolution from the state at 14.8 MeV, which indicates an energy resolution of FWHM = 0.4 MeV (assuming the dominant component is from the experimental resolution and not the intrinsic width). This resolution is consistent with that simulated. Given that the experimental contribution to the excitation energy resolution increases as $\sqrt{E_x - E_{\rm thresh}}$ ($E_{\rm thresh}$ = 12.011 MeV being the decay threshold), the resolution is expected to be ∼0.5 MeV at E_x(^{14}C) = 16 and 0.7 MeV at 21 MeV.

It is of course possible to also extract the excitation energy spectra for the other peaks observed in Fig. 2. However, the excitation energy can only be determined unambiguously if it is known whether the ^{14}C target recoil or the ^{10}Be breakup fragment are excited. The excitation energy spectrum for breakup of ^{14}C to ^{10}Be(2^+) + α is shown in Fig. 4(b) [Fig. 4(a) shows the ^{10}Be$_{\rm gs}$ + α decay]. The decay to ^{10}Be(2^+, 3.37 MeV) proceeds from states at E_x = 17.3, 18.4, (19.0), 19.8, and (21.6) MeV. In the region of overlap between these two spectra there is good agreement between the decay spectra, with the peaks at 17.3 and 18.6 MeV in the ground state decay being found in the decay to the 2^+ state at 17.3 and 18.4 MeV.

For the total energy peak at 79.4 MeV the analysis is a little more complicated owing to the number of possible contributions discussed earlier. To estimate the components from the various possible reactions contributing to this peak we have produced excitation energy spectra gated on the two halves of the peak. The excitation energy spectrum corresponding to the high energy side, which could potentially contain contributions from the decay to the ^{10}Be excited states close to 6 MeV, is shown in Fig. 4(c), shifted assuming the breakup fragment is excited by 5.96 MeV. This shift would

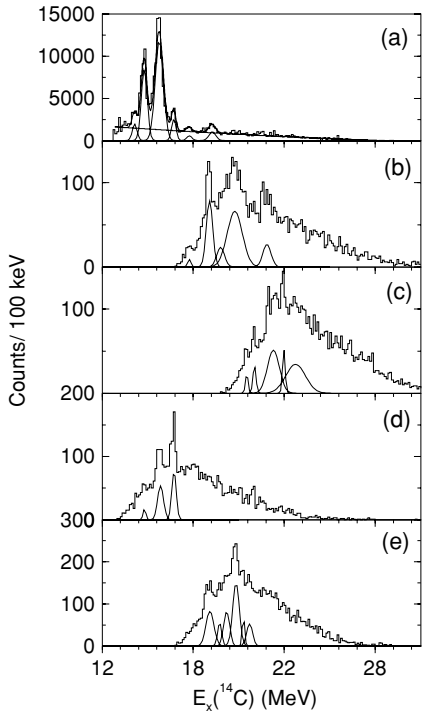

FIG. 4. ^{14}C excitation energy spectrum for the decay to ^{10}Be + α. Also shown are the fits used to extract the peak centroids listed in Table I. Each spectrum was produced by gating on a different region of the total energy spectrum: (a) the peak at 86.2 MeV, (b) the peak at 82.8 MeV, (c) the higher energy side of the 79.4 MeV peak, (d) the lower energy side of the same peak, and (e) the peak at 75.4 MeV.

TABLE I. Summary of the excited states populated in ^{14}C in the ^{14}C(^{14}C,^{14}C* $\rightarrow$ ^{10}Be+α)^{14}C reaction. The table shows the decays for the ^{10}Be ground state in which the ^{14}C recoil is in either the ground state (column 1) or an excited state (column 4). Similarly decays to the ^{10}Be(2$^+$, 3.37 MeV) state are shown in column 2 (for the ^{14}C recoil in the ground state) and column 5 (for the recoil excited state). Decays to the group of ^{10}Be excited states close to 6 MeV are shown in column 3. States that are observed with the greatest strength are shown in bold. Those in brackets represent tentative identifications. The states in column 3, in italics, have an additional uncertainty of up to +300 keV, arising from the uncertainty in the population of the excited state in ^{10}Be.

^{10}Be$_{gs}$ + α	^{10}Be(2$^+$, 3.37 MeV) + α	^{10}Be(6 MeV) + α	^{10}Be$_{gs}$ + α − ^{14}C*	^{10}Be(2$^+$, 3.37 MeV)+α − ^{14}C*
14.3(1)				
14.8(1)			(14.8(1))	
15.6(1)			**15.7(1)**	
16.4(1)			**16.4(1)**	
17.3(1)	17.3(1)			
(18.1)				
18.6(1)	**18.4(1)**			18.4(2)
	(19.0(2))			(19.0(1))
				(19.3(1))
	19.8(1)			**19.8(1)**
		20.4(1)		(20.3(1))
		20.9(1)		20.6(1)
	(21.6(2))	*(21.9(1))*		
		(22.5(1))		
		(23.1(2))		

coincide with the excitation of either the 2$^+$ or 1$^-$ states at this energy. It is possible that the peak corresponds to the excitation of the slightly higher energy 0$^+$ and 2$^-$ states, which would result in the shift being ∼300 keV larger. It is clear that this spectrum is more complex and it is only the dominant strength that has been used for the fits. The spectrum corresponding to the lower energy gate, which should be dominated by excitations of the recoil particle, is shown in Fig. 4(d). It is clear that the two spectra are very different, which would support the hypothesis that Fig. 4(c) contains a dominant component from decays to the ^{10}Be 6 MeV states. The peaks in Fig. 4(d) correlate well with those observed in Fig. 4(a) (Table I). Finally, the data corresponding to the lowest total energy peak, in which both the recoil and breakup nucleus are excited, are shown in Fig. 4(e). In this instance there is no ambiguity, and the decay proceeds to the ^{10}Be(2$^+$, 3.37 MeV) state.

IV. ANGULAR CORRELATION ANALYSIS

The coincident detection of the breakup products of states in ^{14}C permits an analysis of the variation of the decay yield in the ^{14}C center-of-mass frame, as, for example, described in Ref. [9]. Such an analysis can provide information on the spin of the decaying state, but relies on there being a restricted number of reaction amplitudes contributing to the reaction process, as in the case when all entrance and exit channel nuclei are spin-zero. In the present experiment this is the case when all of the final state particles are in their ground states, but not when one or more of them is in an excited state. Thus, such an analysis is restricted to the states observed in Fig. 3.

In the present reaction there are two center-of-mass systems: the first corresponding to the ^{14}C+^{14}C$\rightarrow$^{14}C*+^{14}C inelastic scattering reaction, which may be described in terms of the two angles θ^* and ϕ^*, and the second being the subsequent decay into two ^{10}Be + α, described by the angles ψ and χ (as detailed in Ref. [9]). The angles θ^* and ψ are the polar angles measured with respect to the beam axis and measure the center-of-mass emission angle of the ^{14}C ejectile and the inclination of the ^{10}Be +^{4} He relative velocity vector.

Typically, for reactions involving spin-zero initial and final state particles the number of reaction amplitudes are small and the correlations observed between the two angles θ^* and ψ take the form of a sloping ridge pattern. The periodicity of the ridges is described by a Legendre polynomial of order of the spin of the decaying state, i.e., $P_J(\cos\psi)$. As the dominant orbital angular momenta in the reaction are those corresponding to grazing trajectories, the gradient of the ridges is given by the ratio of the exit channel grazing angular momentum to the spin of the state populated,

$$\frac{\Delta\theta^*}{\Delta\psi} = \frac{J}{l_f} = \frac{J}{l_i - J}, \tag{2}$$

where l_i and l_f are the initial and final state grazing angular momenta. If the "stretched" configuration dominates, which is typically the case for such reactions (see Ref. [9] and references therein), then the entrance and exit channel angular momenta can be related via the expression $l_f = l_i - J$.

The angular correlations therefore provide two signatures of the spin of the decaying ^{14}C state. The periodicity yields a value for J, which should correlate with that extracted from the ridge gradient, assuming that l_i is known. In addition, the value of J extracted from the periodicity should provide a consistent value of l_i for all of the correlations.

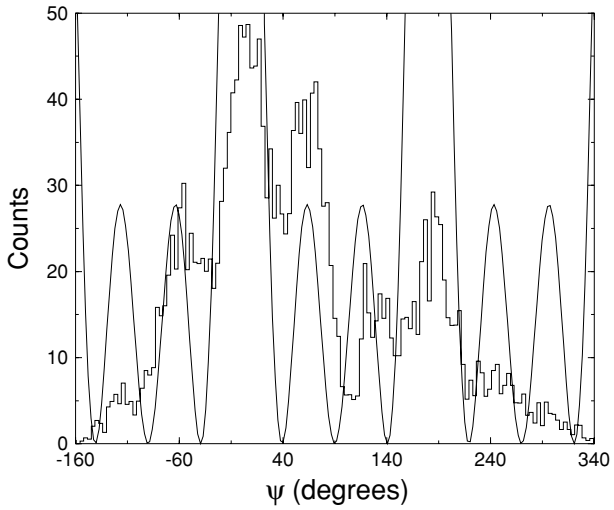

FIG. 5. Projection of the two-dimensional θ^*–ψ data onto the $\theta^* = 0$, ψ axis for the 15.6 MeV state. The data are overlaid with a Legendre polynomial of order 3.

Figure 5 shows the projection of the correlation data onto the $\theta^* = 0$, ψ axis for the 15.6 MeV peak. The periodicity of the data is compared with a Legendre polynomial of order 3. Most of the oscillatory features of the data are reproduced. From the angle of projection [Eq. (2)] it is possible to extract a value for l_i, the entrance channel grazing partial wave. For $J = 3$, this would correspond to $l_i = 24\hbar$. A calculation of the grazing angular momentum of the ^{14}C +^{14} C reaction at the present beam energy gives a value of 25 $\hbar$, i.e., very close to that extracted. This provides an additional level of confidence in a $J^\pi = 3^-$ assignment for this state.

A similar analysis of the other peaks observed in Fig. 3 was performed. However, the correlations were considerably less well determined, and at best only tentative spins or ranges of spins could be deduced: the state at 14.8 MeV may be $J^\pi = 2^+$, and the state at 16.4 $J^\pi = 1^-$ or 3^-. Clearly, the major limitation is the greatly reduced statistics for these states, and higher statistic measurements should be performed. Such measurements are planned for the future.

V. DISCUSSION

The present results for the α decay of ^{14}C to both the ground and 2^+, 3.37 MeV states in ^{10}Be are summarized in Table II, together with other measurements of the spectrum of ^{14}C excited states. These include the α decay following one-neutron transfer using the ^{14}C(^{13}C,^{10}Be + α) reaction [7], α decay of ^{14}C via the ^{7}Li(^{9}Be,^{10}Be + α) reaction [12], states in ^{14}C populated in the same reaction but with the projectile and

TABLE II. Summary of the excited states populated in ^{14}C in the ^{14}C(^{14}C,^{14}C $\rightarrow$ ^{10}Be[0^+(gs), 2^+(3.37 MeV)] + α)^{14}C reaction. A comparison with previous work is also included. States that are populated strongly in the various reactions are shown in bold. It should be noted that there are some differences between the ^{13}C(n, n) data in Ref. [10] (Table V) and Ref. [11] (Table 14.8).

This work		^{14}C(^{13}C,^{10}Be + α) [7]	^{7}Li(^{9}Be,^{10}Be[a]+α) [12]	^{9}Be(^{7}Li, d) [6]	2n transfer [6]		^{13}C(n, n) [10], Table V	
E_x (MeV)	J^π ($\hbar$)	E_x (MeV)	E_x (MeV)	E_x (MeV)	E_x (MeV)	J^π	E_x (MeV)	J^π
14.3(1)								
				14.67	**14.67(5)**	6^+	14.63:14.717	(1^-):4^+
14.8(1)		**14.9(1)**	14.7(1)	**14.87**	**14.87(4)**	5^-	14.91	(1^+)
				15.18			15.20	4^-
15.6(1)	3^-		15.5(1)	15.40			15.55	3^-
					15.75(8)		15.8	(1^-)
		15.9(1)					15.91	4^+[b]
16.4(1)		16.5(1)	**16.4(1)**	**16.43**:16.53	16.4(1)	(6^+)	16.43	
				16.72	**16.72(5)**	(6^-)	16.715	(1^+)
17.3(1)								
				17.30			17.30	4^-
				17.52	17.5(1)		(17.5)	(1^+)
				17.91			17.95	
				18.03			18.10	
18.6(1)		18.5(3)	**18.5(1)**	**18.39**:18.60	18.6(1)			
(19.0(2))		(19.1(2))	(19.1(1))	19.14				
(19.3(1))								
19.8(1)		(19.9(2))	**19.8(1)**	19.73	19.8(1)	(2^+)		
				20.02				
(20.3(1))								
20.6(1)			20.6(1)	20.75		20.4		
				21.00				
21.6(2)		21.3(4)	**21.4(1)**	21.41	21.4(2)			

[a]Decays to both the ^{10}Be ground state and 2^+, 3.37 MeV.
[b]This resonance also appears in the ^{13}C(n, α) channel [10].

target inverted [6], states populated via two-neutron transfer onto ^{12}C [6], and finally neutron resonant scattering on ^{13}C [10]. The ^{9}Be $+^{7}$Li reactions [6,12] have the potential for populating the most complex configurations in ^{14}C given the numbers of particles that must be exchanged between the target and the projectile. In fact, there is some evidence that this reaction proceeds via a compound type mechanism [12].

In general, the spectrum of states observed in the present measurement coincides well with those in the other reactions. There are only a few exceptions. First, in the present work there are two previously unreported states observed, one at 14.3(1) MeV and another at 17.3(1) MeV, that cannot correspond to the 4^- unnatural parity state identified in the ^{13}C(n, n) reaction [10], but is possibly associated with that observed in the ^{9}Be(^{7}Li, d) reaction [6]. Second, there is a marked difference in the excitation of the 15.6 and 15.9 MeV states in the various α-decay studies. In the present inelastic scattering measurements only a state at 15.6 MeV is observed, whereas in the one-neutron transfer study a state appears at 15.9 MeV and in the ^{9}Be $+^{7}$Li reaction a state at 15.5 (15.4) MeV is only relatively weakly excited. An examination of the three spectra associated with the ^{14}C(^{13}C,^{10}Be $+ \alpha$) measurements [7] (reproduced in Fig. 6) suggests that the presence of a state at 15.6 MeV cannot be excluded, because of the finite energy resolution, but that the strength is rather much less than that of the 15.9 MeV state. Conversely, there is little or no evidence for the 15.9 MeV state in the present data. Such a difference must be related to the population mechanism.

The $1n$-transfer reaction (shown in Fig. 6) would strongly populate one-particle states. The inelastic scattering process can excite a whole host of collective states including the $1p$-$1h$ excitations. We can understand the difference in the population of the 15.6 MeV (3^-) state in the above-mentioned reactions if this state has a $\nu p^{-1}_{3/2}$, $\nu d^{1}_{5/2}$ configuration. In this case the 15.6 MeV state cannot be excited via one-nucleon transfer to the ^{13}C ground state and can easily be produced in inelastic scattering with $l = 3$. The fact that the 15.9 MeV state (also seen in the ^{13}C $+ n$ resonant scattering [10] and assigned $J^\pi = 4^+$) is predominantly populated in the $1n$ transfer suggests that this state has a ^{13}C$_{\rm gs} + n$ configuration. Such an excitation would, however, have to be to the fp shell to produce a positive parity state. Indeed, an estimate of the optimum angular momentum for the $1n$ transfer in the ^{13}C $+^{14}$ C interaction, using the Brink matching conditions [13], indicates that the transfer proceeds optimally to an $l =$ 3 orbit. The present data demonstrate that the 15.9 MeV (4^+) state is not strongly excited in the inelastic scattering. At present it is not easy to understand why this might be. It is possible that this arises from kinematics or that ^{14}C ground state and 15.9 MeV excited state are structurally different and the excitation probability is correspondingly reduced.

The otherwise remarkable similarity between the spectra of the α-decaying states in ^{14}C probed, in the different reactions recorded in the first three columns of Table II, is striking. Given the nature of the $1n$ transfer and inelastic scattering excitation mechanisms it is reasonable to speculate that these states have a reasonably strong overlap with the ^{13,14}C ground states. It has been suggested that in this region of excitation energy both prolate and oblate deformed cluster structures should exist [6,14]. As suggested in Ref. [7] it is probable that the present measurements are more strongly associated with oblate type structures.

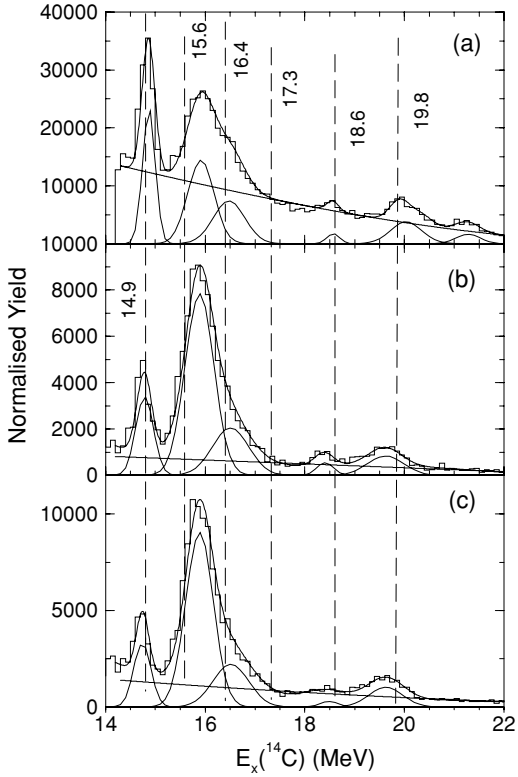

FIG. 6. ^{14}C excitation energy spectra for the ^{14}C(^{13}C,^{10}Be $+ \alpha$) reaction [7] for beam energies of (a) 77.8, (b) 112.25, and (c) 119.25 MeV. The vertical dashed lines indicate the energies of the states from the present measurements (Tables I and II).

VI. SUMMARY

A measurement has been undertaken of the α decay of ^{14}C excited states populated in inelastic scattering from a ^{14}C target. A series of states at 14.3, 14.8 15.6, 16.4, 17.3, 18.6, 19.8, 20.6, and 21.6 MeV was observed to decay to either the ^{10}Be ground (0^+) or first excited (2^+) states. Measurements of the decay fragment angular correlations were used to assign a spin and parity of 3^- to the 15.6 MeV state. The spectrum of states observed in the present measurements is similar, with few exceptions, to those populated in other reactions, for example, $1n$ transfer onto ^{13}C, suggesting that the structures are strongly connected with the ^{13,14}C ground state. Two families of cluster states are predicted in the excitation energy region probed here, with both oblate and prolate characters. If the present states are structurally linked to either of these, then it is probable that the oblate configurations are being probed in the present study. Additional measurements of the spins of the ^{14}C states will be required to firmly establish the cluster systematics in this region. In particular the determination of the spin of the 14.8 MeV state would help link the present measurements to the rotational systematics identified in Ref. [6]. Such measurements are planned for the future.

ACKNOWLEDGMENTS

The authors thank the staff of the IPN Orsay Tandem facility for assistance in running the experiments and the technical staff of LPC-Cean for their assistance in preparing the experiment. We acknowledge the financial support of the U.K. Engineering and Physical Sciences Research Council (EPSRC).

[1] W. von Oertzen *et al*., Phys. Rep. **432**, 43 (2006).
[2] A. Tohsaki, H. Horiuchi, P. Schuck, and G. Ropke, Phys. Rev. Lett. **87**, 192501 (2001).
[3] H. O. U. Fynbo *et al*., Eur. Phys. J. A **15**, 135 (2002).
[4] N. Itagaki, S. Okabe, K. Ikeda, and I. Tanihata, Phys. Rev. C **64**, 014301 (2001).
[5] M. Milin and W. von Oertzen, Eur. Phys. J. A **14**, 295 (2002).
[6] W. von Oertzen *et al*., Eur. Phys. J. A **21**, 193 (2004).
[7] D. L. Price *et al*., Nucl. Phys. **A765**, 263 (2006).
[8] N. Soić *et al*., Nucl. Phys. **A728**, 12 (2003).
[9] M. Freer, Nucl. Instrum. Methods A **383**, 463 (1996).
[10] D. A. Resler, H. D. Knox, P. E. Koehler, R. O. Lane, and G. F. Auchampaugh, Phys. Rev. C **39**, 766 (1989).
[11] F. Ajzenberg-Selove, Nucl. Phys. **A523**, 1 (1991).
[12] N. Soić *et al*., Phys. Rev. C **68**, 014321 (2003).
[13] D. M. Brink, Phys. Lett. **B40**, 37 (1972).
[14] N. Itagaki, T. Otsuka, K. Ikeda, and S. Okabe, Phys. Rev. Lett. **92**, 142501 (2004).